Bayesian Monitoring of Times Between Events: The Shewhart t_r-Chart

NIRPEKSH KUMAR

University of Pretoria, Hatfield, Pretoria, South Africa and Banaras Hindu University, Varanasi, India

SUBHA CHAKRABORTI

University of Alabama, Tuscaloosa, Alabama, USA and University of Pretoria, Hatfield, Pretoria, South Africa

The traditional (frequentist) t_r-chart is a Shewhart-type chart useful for monitoring times between events (interarrival times) following an exponential distribution. This problem often arises in high-yield processes where the defect rate is low and hence the conventional attribute charts such as the c-chart and the u-chart are often ineffective. We consider this problem under the Bayesian framework and propose a Bayesian t_r-chart when the exponential rate parameter is unknown. The Bayesian t_r-chart is a Shewhart-type chart that incorporates parameter uncertainty via a prior and a posterior distribution, unlike the traditional t_r-chart. The control limits are constructed from the predictive distribution of a plotting statistic. The performance of the proposed chart is evaluated and comparisons are made with the traditional t_r-chart. The Bayesian chart is seen to be advantageous in certain situations. An illustrative example is given and a summary and conclusions are offered.

Key Words: Bayesian and Frequentist Control Charts; Exponential Distribution; Performance Metrics; Predictive Distribution; Prior and Posterior Distributions.

1. Introduction

With the increased use of modern technologies in various industries, the defect rate (or the failure rate) in many processes has been decreased to such an extent that the conventional attributes charts for count data are found to be inefficient. For instance, in high-yield processes, due to the process improvements made, there may be many zeros plotted on the traditional p-chart and, hence, the chart becomes uninformative or not useful. In such situations, Montgomery (2012) and others have recommended the use of control charts for monitoring the observed times between consecutive failures instead of the observed number of failures. These control charts based on the times between consecutive failures (interarrival times) are known as times between events (TBE) control charts in the literature. In situations with a low failure rate, a failure can be regarded as a rare event and the occurrence of the event can be modeled by a homogeneous Poisson process with a constant failure rate. Under this assumption, these interarrival times are independent and identically distributed (i.i.d.) exponential random variables with a rate parameter equal to the failure rate of the homogeneous Poisson process. Many TBE control charts (both phase I and phase II charts) have been proposed in the literature: e.g., the exponential chart (Chan et al. (2002), Jones and Champ (2002), Xie et al. (2002), Zhang et al. (2006, 2011), Kumar and Chakraborti (2015)), the cumulative quantity control (Liu et al. (2004, 2006), the exponential cumulative sum chart (CUSUM; Lucas (1985), Vardeman and Ray (1985), Gan (1994), Borror et al. (2003), Zhang et al. (2014), Qu et al. (2015)); the exponentially weighted moving average chart (EWMA; Gan (1998), Ozsan et al. (2010)), and the t_r-chart (Xie et al. (2002), Kumar and Chakraborti (2016)).

Note that several of these charts have been pro-

Dr. Kumar is an Assistant Professor in the Department of Statistics. His email address is nirpeksh@gmail.com. He is the corresponding author.

Dr. Chakraborti is a Professor in the Department of Information Systems, Statistics, and Management Science. His email address is schakrab@cba.ua.edu.

posed for the case when the failure rate is known. In practice, this situation occurs rarely and the rate parameter is often unknown. Recently, the issue of parameter estimation and its effects on various control charts have drawn much attention in the SPC literature. The traditional approach of dealing with parameter estimation in SPC has been to use the frequentist approach (cf., Ghosh et al. (1981), Quesenberry (1993), Chen (1997), Saleh et al. (2013) Zhang et al. (2014), Kumar and Chakraborti (2016)), where a reference sample is used to estimate the unknown parameter(s) and the control limits. Properties of the estimated control limits (and of the resulting control chart) are then studied in terms of the run-length distribution and associated characteristics such as the average run length.

An alternative to the frequentist (classical) approach is to use a Bayesian approach. Here, the parameter is viewed as "a random variable" and is assumed to follow a prior distribution with certain parameters. There has been some work on control charts using a Bayesian approach. A good introduction to the area is the book by Colosimo and del Castillo (2007). Bayesian approaches to SPC and control charts have been considered by Tsiamyrtzis and Hawkins (2007) and Nenes and Tagaras (2007), among others. Woodward and Neylor (1993) developed a Bayesian approach to monitor processes for the production of a small number of items. Arnold (1990) proposed an economic $\overline{X}$-chart for the joint control of the means of independent quality characteristics. Other works include Menzefricke (2002) that incorporated the uncertainty in the parameters into the construction of the control chart limits using a prior distribution. He developed control charts for the mean and the proportions based on the predictive distribution of a plotting statistic and evaluated the chart in terms of predictive average and the predictive standard deviation of the run length. Recently, Raubenheimer and Van der Merwe (2014) constructed control charts for nonconformities (c-chart) using a Jeffreys prior and evaluated chart performance based on the metrics introduced by Menzefricke (2002).

In this paper, we consider the important problem of monitoring the interarrival times following an exponential distribution in the unknown rate parameter case. We focus on the Shewhart-type t_r-chart for this problem, originally proposed by Xie et al. (2002). In generalizing their work to the unknown parameter case, Kumar and Chakraborti (2016) studied the effects of parameter estimation on the t_r-chart, assuming the availability of a phase I reference sample of size m from an in-control (IC) process. As noted earlier, this is the frequentist approach. In this paper, we consider a Bayesian approach and construct a Shewhart-type t_r-chart for the unknown exponential rate parameter. This approach has the intuitive appeal that any available knowledge about the process gained from any past experience can be incorporated into the phase II control charting regime via an assumed prior distribution for the parameter. Control limits can then be constructed based on what is called the predictive distribution of a plotting statistic.

Note that we consider the Shewhart-type t_r-charts here for simplicity and the ease of explaining the basic ideas; other, more sophisticated types of charts such as the CUSUM or the EWMA will be considered elsewhere.

The outline of the paper is as follows. The frequentist control limits of the t_r-chart, starting with the known parameter case, are discussed in Section 2. Then the control limits for the unknown-parameter case are introduced. Next, following this line of thinking, control limits of the Bayesian t_r-chart for the unknown-parameter case are obtained in Section 3. An illustrative example with some real data is given in Section 4. In Section 5, various chart-performance metrics (measures) are introduced to evaluate chart performance, and in Section 6, a simulation study is carried out to examine chart performance, both in the IC and out-of-control (OOC) cases, including comparisons with some existing charts, in terms of these measures. Finally, some concluding remarks are offered in Section 7.

2. Frequentist t_r-Chart in the Known-and Unknown-Parameter Cases

Xie et al. (2002), Cheng and Chen (2011), and others considered the Shewhart-type t-chart for monitoring high-yield processes based on the interarrival times following an exponential distribution. In order to improve the performance of the t-chart, Xie at al. (2002) and Zhang et al. (2007) also considered a generalization, the t_r-chart (also known as a gamma chart), which is based on monitoring the time until the rth failure, which uses more information in the decision-making process. Obviously, taking $r = 1$, we get the t-chart. Let T_r denote the time until the rth failure in a homogeneous Poisson process with a failure rate λ. Thus T_r, being the sum of r i.i.d exp(λ)

TABLE 1. The Chart Design Parameters A_1 and A_2 for the Case K Frequentist t_r-Chart for a Nominal ARL_0 Equal to 370.4

$r=1$		$r=2$		$r=3$	
A_1	A_2	A_1	A_2	A_1	A_2
0.00135	6.60773	0.05288	8.90029	0.21168	10.86962

variables, follows a gamma distribution with parameters r and λ.

In the known-parameter case (hereafter case K), the process is said to be IC when $\lambda = \lambda_0$, where λ_0 is the given (known) or specified value of the rate parameter. The probability control limits for the case K are given in terms of the percentiles of a chi-square distribution as follows:

$$L_r = \frac{\chi^2_{2r,\alpha_0/2}}{2\lambda_0} = \frac{A_1}{\lambda_0} \quad \text{and} \quad U_r = \frac{\chi^2_{2r,1-\alpha_0/2}}{2\lambda_0} = \frac{A_2}{\lambda_0}, \tag{1}$$

where L_r and U_r are the lower and upper control limits, α_0 denotes the nominal false-alarm rate (FAR), and $\chi^2_{2r,\alpha}$ denotes the 100α-percentile of the chi-square distribution with $2r$ degrees of freedom. Note that the constants $A_1 = \chi^2_{2r,\alpha_0/2}/2$ and $A_2 = \chi^2_{2r,1-\alpha_0/2}/2$ in Equation (1) are the chart design parameters for a specified nominal α_0 (which is equal to the reciprocal of the nominal ARL_0 in case K) value. These constants are provided in Table 1 for $\alpha_0 = 0.0027$ (or, $\text{ARL}_0 = 370.4$). The center line (CL) of the control chart is taken to be the median of the distribution of T_r, given by $\text{CL} = \chi^2_{2r,0.5}/(2\lambda_0)$.

In practice, however, the IC value of the parameter λ, i.e., λ_0, is often not known, especially in the start-up phase of a process. This situation is denoted by case U and in this case one approach is to estimate λ using a suitable estimator, say $\hat{\lambda}$, from a phase I reference sample of size m when the process is IC. Then, using $\hat{\lambda}$, the estimated ("plug-in") control limits of the t_r-chart in case U are given by

$$\hat{L}_r = \frac{A_1}{\hat{\lambda}} \quad \text{and} \quad \hat{U}_r = \frac{A_2}{\hat{\lambda}}. \tag{2}$$

Note that the control limits in Equation (2) are random variables, being functions of the estimator $\hat{\lambda}$ and, hence, the usual control chart performance metrics, e.g., the average run length, the false-alarm rate, etc., are all random variables and have their own probability distribution. The uncertainty in the control limits and, consequently in the performance metrics, is introduced and described by the sampling distribution of the estimator $\hat{\lambda}$. For more details, the reader is referred to Kumar and Chakraborti (2016). We refer to this approach of constructing the control limits as the classical (frequentist) approach.

Kumar and Chakraborti (2016) showed that, in case U, using the plug-in limits, that is, replacing the parameters with estimates but using the same A_1 and A_2 values as in case K (see Table 1), the frequentist t_r-chart leads to AARL_{in} (the expected value of the IC conditional ARL, defined in Section 4) values that are less than the nominal ARL_0 for small to medium reference sample sizes. This means that more frequent false alarms are observed than what is nominally expected, especially when a small number of phase I observations are available. Thus, while the plug-in limits can be used, it is more desirable to design the chart (i.e., find the design parameters A_1 and A_2) so that the AARL_{in} of the chart is equal to the nominal ARL_0 for a given phase I sample size m in a specific application. This is generally the notion used in case U, that is, one finds the control limits so that some attribute of the IC run length distribution is controlled, such as the AARL_{in} value being equal to the nominal ARL_0 value.

To this end, we define the modified chart design parameters for the frequentist t_r-chart as

$$A_1^* = \frac{\chi^2_{2r,\alpha_F/2}}{2} \quad \text{and} \quad A_2^* = \frac{\chi^2_{2r,1-\alpha_F/2}}{2}, \tag{3}$$

where the constant α_F (and hence A_1^* and A_2^*) satisfy

$$\text{AARL}_{\text{in}} = \text{ARL}_0 = 370.4, \tag{4}$$

say. Thus, the modified control limits of the frequentist t_r-chart in case U, are given by

$$\hat{L}_r^M = \frac{A_1^*}{\hat{\lambda}} \quad \text{and} \quad \hat{U}_r^M = \frac{A_2^*}{\hat{\lambda}}, \tag{5}$$

where A_1^* and A_2^* are defined in Equation (3). The values of α_F and the modified chart design parameters are presented in Table 2 for different phase I sample size m and a nominal $\text{ARL}_0 = 370.4$ for the frequentist t_r-chart ($r = 1, 2, 3$). These were obtained by solving Equation (4) in MATLAB R2014a. Other

TABLE 2. The Modified Chart Design Parameters A_1^* and A_2^* for the Case U Frequentist t_r- Chart for a Nominal ARL_0 Equal to 370.4

	$r=1$			$r=2$			$r=3$		
m	α_F	A_1^*	A_2^*	α_F	A_1^*	A_2^*	α_F	A_1^*	A_2^*
30	0.00248	0.00124	6.69143	0.00229	0.04862	9.08410	0.00212	0.19462	11.15648
40	0.00253	0.00127	6.67326	0.00236	0.04943	9.04785	0.00222	0.19766	11.10345
50	0.00256	0.00128	6.66162	0.00242	0.04997	9.02389	0.00229	0.19974	11.06776
60	0.00258	0.00129	6.65351	0.00245	0.05037	9.00678	0.00234	0.20126	11.04189
70	0.00259	0.00130	6.64753	0.00248	0.05066	8.99392	0.00238	0.20243	11.02220
80	0.00261	0.00130	6.64294	0.00250	0.05090	8.98387	0.00241	0.20335	11.00667
90	0.00262	0.00131	6.63930	0.00252	0.05109	8.97580	0.00243	0.20410	10.99409
100	0.00262	0.00131	6.63633	0.00254	0.05124	8.96917	0.00245	0.20472	10.98367
150	0.00265	0.00132	6.62721	0.00259	0.05173	8.94823	0.00252	0.20674	10.95024
200	0.00266	0.00133	6.62250	0.00261	0.05200	8.93709	0.00256	0.20784	10.93209
250	0.00267	0.00133	6.61962	0.00263	0.05216	8.93017	0.00259	0.20854	10.92065
300	0.00267	0.00134	6.61768	0.00264	0.05228	8.92544	0.00260	0.20902	10.91277
350	0.00268	0.00134	6.61629	0.00265	0.05236	8.92201	0.00262	0.20937	10.90701
400	0.00268	0.00134	6.61524	0.00265	0.05242	8.91940	0.00263	0.20964	10.90260
450	0.00268	0.00134	6.61441	0.00266	0.05247	8.91735	0.00263	0.20986	10.89913
500	0.00268	0.00134	6.61375	0.00266	0.05251	8.91570	0.00264	0.21003	10.89633
1,000	0.00269	0.00135	6.61068	0.00268	0.05269	8.90803	0.00267	0.21084	10.88321

nominal ARL_0 values, such as 500, can also be used if desired.

From Tables 1 and 2, it can be seen that, for $m \geq 500$, the α_F values are closer to $1/ARL_0 = 0.0027$ and, hence, the constants A_1^* and A_2^* are closer to the values of A_1 and A_2 (constants for case K) and they converge to A_1 and A_2, respectively, as $m \to \infty$. But for small to moderate values of m, which may be more reasonable to occur in practice, the charting constants A_1^* and A_2^* should be used to construct the frequentist t_r-charts in case U.

As noted earlier, an alternative approach to monitoring in SPC is to use the Bayesian approach. This involves accommodating the uncertainty in the estimation of λ, using a prior and a posterior distribution (of λ), and constructing the control limits for the t_r-chart (in case U) using the predictive distribution of the plotting statistic for the future (phase II) sample of observations. This is outlined now.

3. Bayesian t_r-Chart in the Unknown-Parameter Case

Menzefricke (2002) proposed a method for obtaining the control limits for the normal mean in both the standard deviation known and unknown cases, using a Bayesian approach, based on the predictive distribution of the plotting statistic from a future sample. In this setup, he also sketched a general algorithm for obtaining the control limits based on the predictive density. We follow this approach for the t_r-chart by incorporating two sources of information about the parameter λ: an assumed prior distribution and the information from a phase I reference sample obtained from an IC process.

To fix ideas, let X denote the interarrival time in a homogeneous Poisson process with rate λ. Suppose that X has a probability density function (pdf) $f(x \mid \lambda)$. In the Bayesian approach, we assume that we have some prior knowledge or information about λ, which can be summarized by a prior pdf. In particular, we assume a gamma family of prior distributions for λ, with shape parameter a and scale parameter b, denoted by $\Gamma(a, b)$. The gamma distribution is in fact known as the "conjugate" prior for λ, which is widely used in the Bayesian literature. We further assume that a phase I reference sample $x_1, x_2, \ldots, x_m$ of size m is available after a phase I analysis, from an IC process, with the pdf $f(x \mid \lambda)$ having exponential distribution $\exp(\lambda)$. In this setting, it is well known that the posterior distribution of λ itself is a gamma distribution with shape parameter $(a + m)$

and scale parameter $(b+y)$, i.e., $\Gamma(a+m, b+y)$ (see Gelman (2002), Colosimo and dell Castillo (2007)). This is one advantage of using a conjugate prior distribution.

Note that the mean of the posterior distribution of λ is $(a+m)/(b+y)$. When $a \to 0$ and $b \to 0$, the limiting prior distribution becomes proportional to $1/\lambda$, which corresponds to the Jeffreys prior (which is a noninformative prior as well as an improper prior because the total area under the distribution is not equal to 1). However, this does not affect any of the inferences with respect to the posterior distribution and the predictive density. Note that Jeffreys prior is proportional to $\sqrt{\det(I(\lambda))}$, where $\det(I(\lambda))$ is the determinant of Fisher's information, which is $1/\lambda^2$ in this case. However, interestingly, the posterior mean equals $m/y = 1/\bar{x}$, which is the maximum likelihood estimator (MLE) of λ in the frequentist approach. Henceforth, this limiting prior distribution will be denoted by $\Gamma(0,0)$ and will be referred to as the case $a \to 0$, $b \to 0$.

The frequentist t_r-chart is based on the plotting statistic T_r, the waiting time until the rth failure, that is the sum of the r interarrival times in a prospective (or phase II) sample being monitored. The Bayesian t_r-chart also uses the same plotting statistic but the control limits are found using the predictive distribution of T_r. For a given r and a given observed value of $Y = y$ (obtained from the reference sample), the predictive density function of T_r is equal to

$$\begin{aligned} f_{T_r|y}(t) &= \int_0^\infty f_{T_r}(t \mid \lambda) p(\lambda \mid y) d\lambda \\ &= \int_0^\infty \frac{\lambda^r}{\Gamma(r)} t^{r-1} e^{-\lambda t} \\ &\qquad \times \frac{(b+y)^{a+m}}{\Gamma(a+m)} \lambda^{a+m-1} e^{-(b+y)\lambda} d\lambda \\ &= \frac{(b+y)^{a+m}}{B(a+m,r)} \frac{t^{r-1}}{(t+b+y)^{a+m+r}}; \quad t > 0, \end{aligned} \tag{6}$$

where $B(a,b) = \Gamma(a)\Gamma(b)/\Gamma(a+b)$ is the beta function. The $f_{T_r}(t \mid \lambda)$ is $\Gamma(r,\lambda)$, the pdf of T_r, and $p(\lambda \mid y)$ is $\Gamma(a+m, b+y)$, the pdf of the posterior distribution of λ.

The predictive distribution of T_r given in Equation (6) is used to calculate the control limits L_r^* and U_r^* for the proposed Bayesian t_r-chart, to monitor the unknown process parameter λ, in phase II. Thus, using Equation (6), one can set

$$P[T_r < L_r^* \mid Y = y] = \frac{\alpha_B}{2}$$

and

$$P[T_r > U_r^* \mid Y = y] = \frac{\alpha_B}{2}$$

and find the upper and lower (predictive) control limits of a Shewhart-type chart so that the AARL_{in} is equal to some nominal ARL_0. It is emphasized that basing the control chart on the predictive distribution of T_r formally incorporates the knowledge about the parameter λ through the assumed prior distribution and the available reference sample. Also, as is typically done in the literature, in case U, we find the control limits for a given nominal ARL_0.

Further, letting

$$W_r = (b+y)/(T_r + b + y),$$

it can be shown that W_r follows a beta distribution with parameters $(a+m)$ and r and hence the lower and the upper control limits L_r^* and U_r^* can be expressed in terms of the percentiles of the more familiar beta distribution with parameters $a+m$ and r, given by

$$L_r^* = (b+y)\left(\frac{1}{B_{1-\alpha_B/2}(a+m,r)} - 1\right)$$

and

$$U_r^* = (b+y)\left(\frac{1}{B_{\alpha_B/2}(a+m,r)} - 1\right), \tag{7}$$

where $B_c(\beta_1, \beta_2)$ denotes the $100c$-percentile of a beta distribution with parameters β_1 and β_2. The center line of the chart is taken to be the median of the predictive density of T_r, i.e., C_r^* such that $P[T_r < C_r^*] = 0.5$, which yields

$$C_r^* = (b+y)\left(\frac{1}{B_{0.5}(a+m,r)} - 1\right).$$

Hence the limits in Equation (7) can be written as

$$L_r^* = (b+y)B_1 \text{ and } U_r^* = (b+y)B_2, \tag{8}$$

where the chart design parameters B_1 and B_2 for the Bayesian t_r-chart are given by

$$B_1 = \frac{1}{B_{1-\alpha_B/2}(a+m,r)} - 1$$

and

$$B_2 = \frac{1}{B_{\alpha_B/2}(a+m,r)} - 1. \tag{9}$$

The constant α_B and hence B_1 and B_2 are obtained so that the chart attains the expected value of condi-

TABLE 3. The Chart Design Parameters α_B, B_1 and B_2 for the Bayesian t_r-Chart for Different Values of r, $a + m$ and a Nominal $\text{ARL}_0 = 370.4$

	$r = 1$			$r = 2$			$r = 3$		
$a + m$	α_B	B_1	B_2	α_B	B_1	B_2	α_B	B_1	B_2
20	0.00339	0.00008	0.37567	0.00359	0.00299	0.52076	0.00388	0.01153	0.64570
30	0.00321	0.00005	0.23925	0.00332	0.00193	0.32900	0.00347	0.00749	0.40672
40	0.00310	0.00004	0.17551	0.00318	0.00142	0.24026	0.00328	0.00555	0.29639
50	0.00304	0.00003	0.13860	0.00309	0.00112	0.18918	0.00317	0.00440	0.23302
60	0.00299	0.00002	0.11453	0.00304	0.00093	0.15601	0.00309	0.00365	0.19194
70	0.00295	0.00002	0.09759	0.00299	0.00079	0.13273	0.00304	0.00311	0.16316
80	0.00293	0.00002	0.08501	0.00296	0.00069	0.11549	0.00300	0.00271	0.14188
90	0.00290	0.00002	0.07531	0.00293	0.00061	0.10222	0.00296	0.00241	0.12550
100	0.00289	0.00001	0.06760	0.00291	0.00055	0.09168	0.00294	0.00216	0.11252
150	0.00283	0.00001	0.04471	0.00285	0.00036	0.06051	0.00286	0.00143	0.07414
200	0.00280	0.00001	0.03341	0.00281	0.00027	0.04515	0.00282	0.00107	0.05529
250	0.00278	0.00001	0.02666	0.00279	0.00021	0.03602	0.00280	0.00085	0.04408
300	0.00277	0.00000	0.02219	0.00278	0.00018	0.02995	0.00278	0.00071	0.03665
350	0.00276	0.00000	0.01900	0.00277	0.00015	0.02564	0.00277	0.00061	0.03136
400	0.00275	0.00000	0.01661	0.00276	0.00013	0.02241	0.00276	0.00053	0.02741
450	0.00275	0.00000	0.01475	0.00275	0.00012	0.01990	0.00276	0.00047	0.02434
500	0.00274	0.00000	0.01327	0.00275	0.00011	0.01790	0.00275	0.00043	0.02189
1,000	0.00272	0.00000	0.00662	0.00272	0.00005	0.00893	0.00273	0.00021	0.01091

tional average run length equal to the nominal value of ARL_0 when the process is IC.

In Appendix C, it is shown that the various performance metrics depend only on α_B and $(a + m)$. Hence, the chart design parameters B_1 and B_2 are the functions of $(a + m)$ for a given nominal ARL_0. Hence, the chart design parameters B_1 and B_2 in Equation (9) are calculated for a given $(a + m)$ and a nominal ARL_0. These constants are calculated and given in Table 3 for $\text{ARL}_0 = 370.4$.

It can be observed from Table 3 that the constant α_B is a decreasing function of $(a + m)$ for a given ARL_0 and converges to $1/(\text{ARL}_0) = 0.0027$ (the FAR in case K) as $(a + m) \to \infty$. Note that the design parameters B_1 and B_2 are also decreasing functions of $(a+m)$. Table 3 can be useful in implementing the proposed chart in practice.

Thus, operationally, for the proposed Shewhart-type Bayesian t_r-chart, for a selected value of r and for given values of a, b (specifying the prior distribution) and y (obtained from the phase I sample), one calculates the statistic T_r from a phase II sample (that is being monitored) and plots it against the control limits given in Equation (8). If T_r plots outside the control limits, the process is OOC and a search for assignable causes gets underway. Otherwise, the process is declared IC and monitoring moves on to the next sample.

To get some further insights, note that, when $a \to \infty$ such that the mean of the prior distribution, a/b tends to some value λ_0, it is shown in the Appendix B (Theorem 1) that the predictive density of $2\lambda_0 T_r$ converges to the chi-square distribution with $2r$ degrees of freedom. Also, as $a \to \infty$ (hence, $a + m \to \infty$), the α_B converges to $1/\text{ARL}_0$ and, hence, in this case, the Bayesian control limits converge to the control limits for the case when the rate parameter is known and is equal to λ_0 (shown in Appendix B) with $\text{FAR}=1/\text{ARL}_0$. Also, it is shown (see Appendix B, Theorem 2) that, as $m \to \infty$, the predictive density of $2\lambda T_r$ converges to the chi-square distribution with $2r$ degrees of freedom. Because, when $m \to \infty$, the MLE $\hat{\lambda} \to \lambda$, it follows that, as $m \to \infty$, the frequentist t_r-chart control limits based on the distribution of $2\lambda T_r$ (shown in Equation (5)) and the Bayesian control limits based on the predictive distribution of T_r (shown in Equation (8)) both converge to the control limits in the known parameter case (case K), with $\text{FAR}=1/\text{ARL}_0$. Intuitively,

this means that the larger the phase I (reference) sample size, the smaller the difference between the Bayesian and frequentist control limits for λ.

4. Example

In order to illustrate the proposed Bayesian t_r-chart, we consider an example with some real data and contrast the findings with those for the frequentist t_r-chart. The data comprises the recorded time intervals (in days) between coal-mining disasters in England, from 15 March, 1851 to 22 March, 1962 and have been used in the literature for illustration of various procedures. The slightly corrected data, consisting of 190 observations, are provided in Jarrett (1979) and are shown in Table 4 for convenience. The underlying distribution of the interarrival times has been tested to follow an exponential distribution and we monitor the unknown rate parameter λ of this distribution.

A prior distribution is necessary for implementing the Bayesian chart. The choice of a prior distribution is somewhat subjective and has been a matter of debate for a long time (Berger (1985), Gelman (2002), Bayarri (2012)). We illustrate some options here. Recall that, in this paper, we consider the $\Gamma(a, b)$ family of prior distributions, which is known to be a conjugate family. If the practitioner is confident that the parameter λ is close to the mean of the prior distribution, namely, a/b, then it is customary that the variance of the prior distribution, a/b^2, be made small, so that the variance of the posterior distribution of λ is small (Gelman (2002), Kass and Wasserman (1996)). On the other hand, if the practitioner is not very confident that λ is close to a/b, then a diffused or a vague prior is preferred by taking the variance a/b^2 to be large. For large values of the prior variance, both a and b tend to zero, in which case, as shown earlier, the posterior mean tends to the MLE $\hat{\lambda}$ and the control limits tend to become close to the control limits for the case of the noninformative prior.

For illustration, first consider $r = 1$ and the corresponding t_1-chart. Cowles (2013) describes several ways to choose the parameters of a prior distribution in order to express prior beliefs about an unknown parameter. For example, suppose we use the first three observations of the Jarrett (1979) data to set up a $\Gamma(a, b)$ prior distribution of λ. Thus, we set the mean of the prior gamma distribution, a/b to be equal to 0.01064, which is the reciprocal of the average of the first three observations (mean time between failures). Then we consider the next 27 observations as a phase I sample of size $m = 27$, which is used to summarize the current information about the unknown λ. The choice of a and b is not unique from the equation $a/b = 0.01064$, however and so

TABLE 4. Time Intervals in Days Between Explosions in Mines, from March 15, 1851 to March 22, 1962 (to Be Read Down Columns), Reproduced from Jarrett (1979)

157	65	53	93	127	176	22	1,205	1,643	312
123	186	17	24	218	55	61	644	54	536
2	23	538	91	2	93	78	467	326	145
124	92	187	143	0	59	99	871	1,312	75
12	197	34	16	378	315	326	48	348	364
4	431	101	27	36	59	275	123	745	37
10	16	41	144	15	61	54	456	217	19
216	154	139	45	31	1	217	498	120	156
80	95	42	6	215	13	113	49	275	47
12	25	1	208	11	189	32	131	20	129
33	19	250	29	137	345	388	182	66	1,630
66	78	80	112	4	20	151	255	292	29
232	202	3	43	15	81	361	194	4	217
826	36	324	193	72	286	312	224	368	7
40	110	56	134	96	114	354	566	307	18
12	276	31	420	124	108	307	462	336	1,358
29	16	96	95	50	188	275	228	19	2,366
190	88	70	125	120	233	78	806	329	952
97	225	41	34	203	28	17	517	330	632

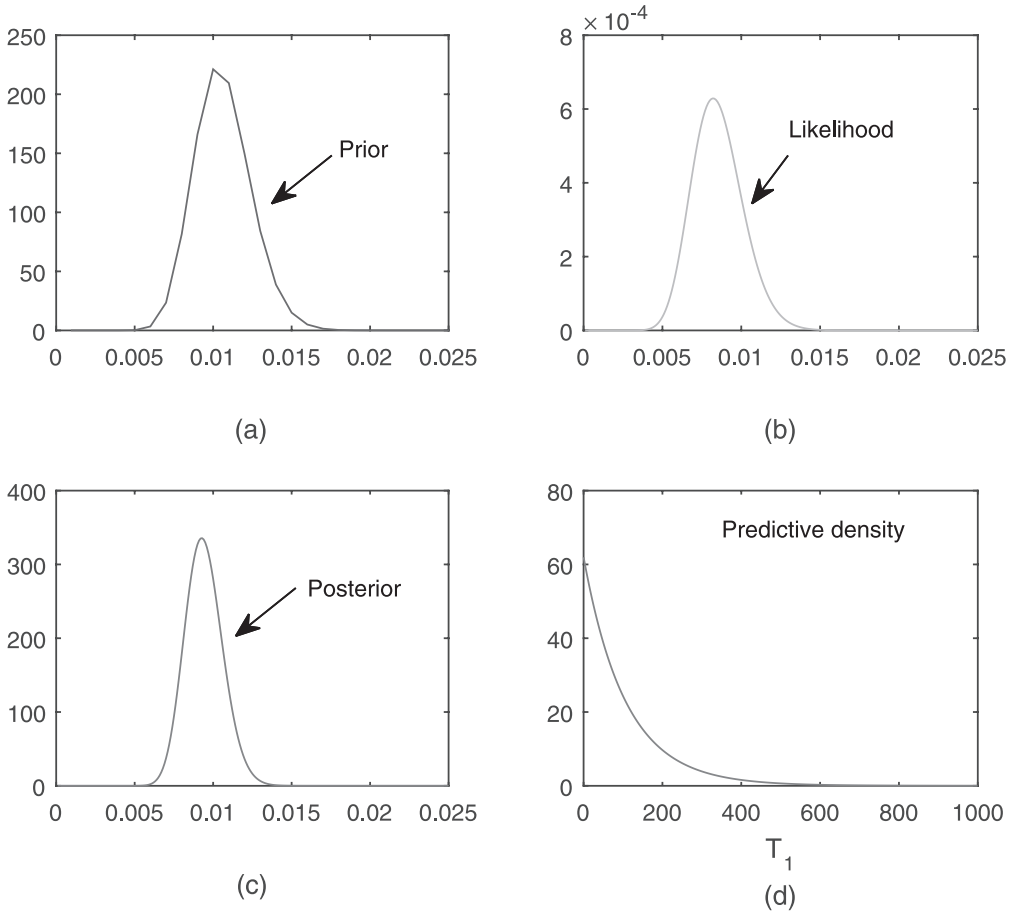

FIGURE 1. The Graphs for (a) the Density of $\Gamma(35, 3295)$ Prior, (b) Likelihood Function with $m = 27$ and $y = 3286$, (c) the Density of Posterior Distribution, and (d) the Predictive Density of T_1.

here, for the purpose of illustration, we select a and b such that the posterior mean $(a + m)/(b + y)$ lies halfway between the prior mean (0.01064) and the MLE of λ ($\hat{\lambda} = 0.0082$) calculated from the 27 phase I observations. This is done so that the posterior pdf reflects both the data (likelihood) and the prior (see Figure 1) distributions more or less equally. It is easy to see that these two choices, i.e., $a/b = 0.01064$ and $(a + m)/(b + y) = 0.00943$ with $y = 3286$, yield, approximately, $a = 35$ and $b = 3295$, so that the prior distribution is a $\Gamma(35, 3295)$ distribution for the parameter λ. Note that other measures of centrality, such as the median (which is a more reasonable measure of location for a skewed distribution) may be preferred to the mean while finding a and b. However, the standard Bayesian analysis under the squared error loss function yields the mean as the estimator and this is what is used here.

Figure 1 shows the graphs of (i) the pdf of the prior distribution of λ: $\Gamma(35, 3295)$; (ii) the likelihood function using the 27 observations taken as the phase I reference sample, which yields $y = 3286$; (iii) the pdf of the corresponding posterior distribution of λ, which is a $\Gamma(35+27 = 62, 3295+3286 = 6581)$ distribution; and (iv) the pdf of the predictive distribution of the plotting statistic T_1. Note that the variance of the posterior distribution is equal to 1.4315×10^{-6} $(= (a+m)/(b+y)^2)$, which is smaller than both the prior variance 3.2237×10^{-6} $(= a/b^2)$ and the estimated variance of the MLE $\hat{\lambda}$, namely, 7.5719×10^{-5} $(= \hat{\lambda}m^2/[(m-1)(m-2)])$.

The Bayesian t_1-chart corresponding to the $\Gamma(35, 3295)$ prior and for a nominal $\mathrm{ARL}_0 = 370.4$ is shown in Figure 2 with the lower and the upper control limits (solid lines; using Equations (8) and (9)) at 0.1583 and 728.4266, respectively. The center line is the median of the predictive density, which is found to be 73.9870. The modified control limits of the fre-

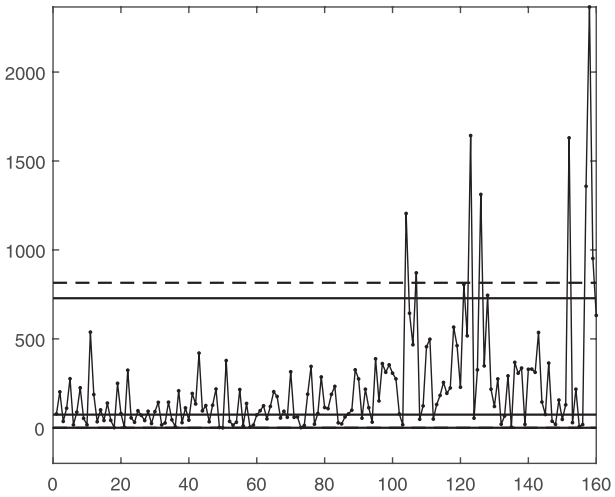

FIGURE 2. The Frequentist t_1-Chart (Dotted Lines) and the Bayesian t_1-Chart (Solid Lines) Using a $\Gamma(35,\ 3295)$ Prior for the Last 160 Observations of the Jarrett (1979) Data.

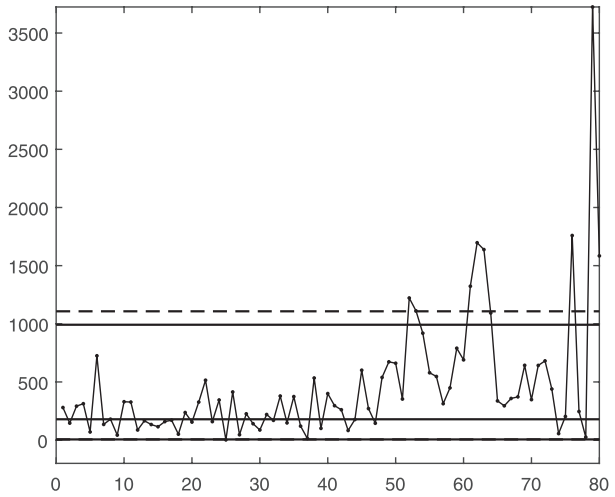

FIGURE 4. The Frequentist t_2-Chart (Dotted Lines) and the Bayesian t_2-Chart (Solid Lines) Using a $\Gamma(35,\ 3295)$ Prior for the Last 160 Observations (80 Charting Statistics) of the Jarrett (1979) Data.

quentist t_1-chart are also shown in the same figure with dotted lines for which the lower and upper control limits are 0.1500 and 815.3023, respectively, for a nominal $\mathrm{ARL}_0 = 370.4$ using Equation (5). It may be noted that using Equation (2) and $\alpha_0 = 0.0027$, as in Kumar and Chakraborti (2016), the frequentist control limits were found to be 0.1644 and 804.1755, respectively. Thus, the two sets of frequentist control limits, used in case U, are slightly different. From Figure 2, it can be seen that the Bayesian control limits are narrower than the frequentist control limits and thus the new charts are expected to be more sensitive to a shift in λ.

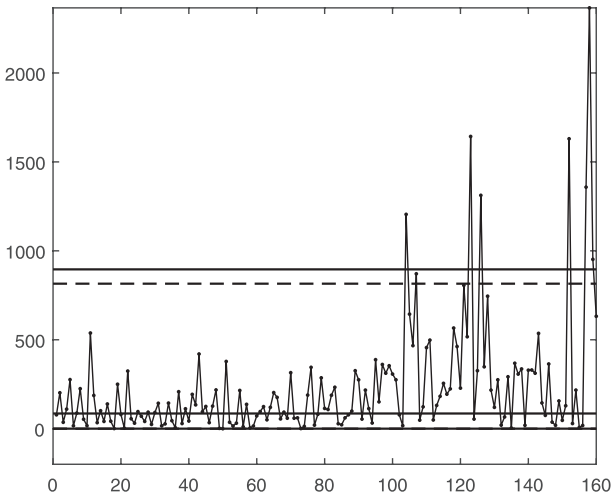

FIGURE 3. The Frequentist t_1-Chart (Dotted Lines) and the Bayesian t_1-Chart (Solid Lines) Using the Noninformative Prior $\Gamma(0,\ 0)$, for the Last 160 Observations of the Jarrett (1979) Data.

If no prior information is available, we may use the noninformative (Jeffreys) prior with $a = 0, b = 0$, i.e., the $\Gamma(0, 0)$ prior. The control chart corresponding to this prior is shown in Figure 3 with the lower and upper control limits (solid lines) at 0.1980 and 882.3040, respectively. Observe that, in this case, the Bayesian control limits are wider than those for the frequentist t_1-chart (dotted lines). This observation is perhaps intuitive and agrees with the results of Menzefricke (2002) and Raubenheimer and van der Merwe (2015).

Finally, consider $r = 2$ and the corresponding Bayesian t_2-chart. Recall that the frequentist t_2-chart was considered to improve performance over the t_1-chart (Xie et al. (2002), Kumar and Chakraborti (2016)), as the T_2-charting statistic is based on the sum of two observations (two consecutive interarrival times) and thus utilizes more information in the decision-making process (than the t_1-chart). The control limits for the Bayesian t_2-chart using the $\Gamma(35, 3295)$ prior are calculated for $m = 27$ and a nominal $\mathrm{ARL}_0 = 370.4$ using Equation (8). The lower and upper control limits and the center line are 5.9050, 991.8654, and 179.1264, respectively, and are shown in Figure 4 with solid lines. For compar-

ison, the control limits for the frequentist t_2-chart are calculated using Equation (5) to be 5.8768 and 1107.3630, respectively, and are also shown in the Figure 4 with dotted lines. It can be seen that the Bayesian t_2-chart using the $\Gamma(35, 3295)$ prior has narrower control limits than the frequentist t_2-chart, which again means a more sensitive chart. Also, as might be expected, the Bayesian t_2-chart using the $\Gamma(35, 3295)$ prior is more sensitive than the Bayesian t_1-chart using the $\Gamma(35, 3295)$ prior to possible shifts in the rate parameter. For example, the 61st plotting statistic (the sum of the 121nd and the 122th observations, 644 and 467, respectively) on the chart is outside of the control limits of the Bayesian t_2-chart using the $\Gamma(35, 3295)$ prior. However, the Bayesian t_1-chart using the $\Gamma(35, 3295)$ prior does not signal on either data point and is thus unable to detect a change in the process at this stage.

5. Chart-Performance Evaluation

The performance of the proposed Bayesian t_r-chart is of interest. We examine this aspect in this section and compare it with the performance of the corresponding frequentist t_r-chart. Typically, the performance of a control chart is evaluated in terms of the first two moments of the run-length distribution. Note that we developed the control chart using the Bayesian approach in Section 3; however, to evaluate the chart performance, we use the frequentist (sampling theory) approach under various hypothetical situations. To this end, suppose that observations (interarrival times) are taken repeatedly from an exponential pdf $f(x \mid \lambda_1)$, where $\lambda_1 = \delta\lambda$ and δ is used to denote a possible amount of shift in the unknown rate parameter λ. If in phase II, $\delta = 1$, the process is IC, otherwise $\delta \neq 1$ and the process is out-of-control (OOC). If $\delta > 1$, the process deteriorates because the mean time to failure decreases, whereas, for $\delta < 1$, the process improves as the mean time to failure increases. Clearly, the case $\delta > 1$ deserves more serious attention in practice.

Recall that the original plotting statistic T_r follows a gamma distribution with parameters r and λ_1. Hence, the probability of a signal in phase II is given by

$$\begin{aligned}\beta(\lambda_1) &= P[T_r < L_r^* \text{ or } T_r > U_r^* \mid \lambda_1] \\ &= 1 + G_{\chi^2_{2r}}(2\lambda_1 L_r^*) - G_{\chi^2_{2r}}(2\lambda_1 U_r^*).\end{aligned}$$

This follows from the fact that $2\lambda_1 T_r$ follows a chi-square distribution with $2r$ degrees of freedom and $G_{\chi^2_{2r}}(\cdot)$ denotes its cumulative distribution function (cdf). Note that the probability of a signal is a conditional probability that depends on nominal ARL_0, y, a, b, m, and δ for a given λ_1. Hence, for a given λ_1, or conditionally on λ_1 (this is a random variable in the Bayesian setting), the run length variable R, in phase II, follows a geometric distribution with parameter $\beta(\lambda_1)$. Thus, again, note that the conditional run length distribution depends on L_r^* and U_r^* for a given λ_1 or, in turn, on ARL_0, y, a, b, m, and δ for a given λ. Hence, the first two moments of the conditional run length distribution are

$$\text{E}[R \mid \lambda_1] = \text{E}[R \mid \lambda] = \text{CARL} = \frac{1}{\beta(\lambda_1)} = \frac{1}{\beta(\delta\lambda)} \tag{10}$$

and

$$\text{E}[R^2 \mid \lambda_1] = \text{E}[R^2 \mid \lambda] = \frac{2 - \beta(\delta\lambda)}{\beta^2(\delta\lambda)}$$

because $\lambda_1 = \delta\lambda$. $\text{CARL}=1/\beta(\delta\lambda)$ is the expected value of conditional run length distribution and depends on ARL_0, y, a, b, m, and δ for a given λ.

To evaluate the chart performance, Menzefricke (2002) used two metrics, namely, the *predictive* mean and the predictive standard deviation of the run-length distribution. These are given by

$$\int_0^\infty \left[\frac{1}{\beta(\delta\lambda)}\right] p(\lambda \mid y) d\lambda \tag{11}$$

$$\sqrt{\text{E}[E[R^2 \mid \lambda]] - [\text{E}[\text{E}[R \mid \lambda]]]^2}, \tag{12}$$

respectively. Note that, in expression (12), the second expectation is over the distribution of random variable conditional run length and the first expectation is taken over the posterior distribution of λ.

The metrics (11) and (12) are discussed by Menzefricke (2002) when $\delta = 1$, i.e., for the IC process. Note that these are primarily unconditional performance measures that are obtained by averaging the conditional measures over the posterior distribution of λ. However, as noted in the recent literature, the conditional measures have some important advantages while developing a better understanding about the performance of the chart in practice. Recently, in the classical setting, Jones and Steiner (2012) proposed a metric that is the standard deviation of the distribution of the conditional ARL (CARL), to examine the variability in the CARL distribution via the sampling distribution of the estimator $\hat{\lambda}$. Later, Kumar and Chakraborti (2016) used this metric to better understand the practitioner-to-practitioner variability in the CARL distribution, which varies for each reference sample taken from an IC process. In the Bayesian setting, we may also use the aforementioned

concept to study the variability in CARL distribution via the posterior distribution of λ.

As noted earlier, the posterior distribution incorporates both the prior information and the information supplied by the phase I sample. Thus, in the Bayesian context, the standard deviation of the CARL reflects both the uncertainty in λ and the phase I reference data at hand (which varies from practitioner to practitioner). Hence, the study of the variability in the CARL distribution, in addition to just the mean, is important. Of course, lower variability is more desirable. Accordingly, we define the following two measures, which are the expected value and the standard deviation of the distribution of the CARL, respectively. Thus,

$$\text{AARL} = \text{E}(\text{CARL}) = \int_0^\infty \frac{1}{\beta(\delta\lambda)} p(\lambda \mid y) d\lambda$$

and

$$\text{SD}_{\text{CARL}} = \sqrt{\text{E}[\text{CARL}^2] - [\text{E}[\text{CARL}]]^2}, \qquad (13)$$

where

$$\text{E}[\text{CARL}^2] = \int_0^\infty \frac{1}{\beta^2(\delta\lambda)} p(\lambda \mid y) d\lambda.$$

Note that the AARL is the predictive mean proposed by Menzefricke (2002). However, the predictive standard deviation in Equation (12) reflects the variability in the conditional run-length distribution, whereas the metric in Equation (13) reflects the variability in conditional average run length distribution. Note that, for the IC case, these measures can all be calculated by letting $\delta = 1$ and the corresponding values are denoted by AARL_{in} and $\text{SD}_{\text{CARL:in}}$, respectively.

Next, we examine the performance of the Bayesian t_r-chart.

6. Performance Results and Discussion

In this section, we first examine the IC performance of the proposed Bayesian t_r-chart and compare it with the frequentist t_r-chart for the unknown parameter case. Then we compare the OOC performance of both the charts for different size shifts in the rate parameter λ.

6.1. In-Control Chart-Performance Evaluation

It is shown in Appendix C that the performance metrics in Equations (11)–(13) do not depend on λ, the sufficient statistic Y (obtained from the reference sample of size m) and b, the scale parameter of the gamma prior distribution but only on the nominal ARL_0, δ, and the sum $(a+m)$. Note that the value of δ needs to be specified to indicate whether or not the process is IC ($\delta = 1$) and, if not, the amount of the shift in the parameter λ ($\delta \neq 1$). First, we consider the case of the noninformative prior ($a = 0$, $b = 0$) in the context of the performance of the Bayesian t_r-chart. To this end, the values of the AARL_{in} and the $\text{SD}_{\text{CARL:in}}$ are calculated and reported, in Table 5, in bold letters corresponding to $\delta = 1$, for different values of m for the t_r-chart, for $r = 1$, 2, and 3, and for a nominal $\text{ARL}_0 = 370.4$. The last block of rows (denoted $m \to \infty$) in Table 5, for each r, displays the values of the metrics when the process parameter is known. All calculations are done in MATLAB R2014a.

Because both charts are designed for the same nominal ARL_0 value of 370.4 for each m, the discussion is focused on the examination of the metric $\text{SD}_{\text{CARL:in}}$. As we discussed earlier, the $\text{SD}_{\text{CARL:in}}$ reflects the variability in the CARL when the process is IC and, hence, it is desirable that it be low so that the chart could be more predictable for a practitioner. It can be observed from Table 5 that both the charts have quite large $\text{SD}_{\text{CARL:in}}$ values for smaller values of m but these converge to zero as m increases. It is worth noting here that, for smaller values of m, the Bayesian t_r-chart has much smaller $\text{SD}_{\text{CARL:in}}$ values than the frequentist t_r-chart, which implies that, for smaller values of m (which is practically important, even more so for the TBE control chart), the Bayesian t_r-chart gives more confidence to the practitioners in their AARL_{in} values than the frequentist t_r-chart. For example, for $m = 20$, the $\text{SD}_{\text{CARL:in}}$ value is 112.9 for the Bayesian t_1-chart, whereas it is 170.3 for the frequentist t_1-chart. Also, it is seen that, as r increases, the $\text{SD}_{\text{CARL:in}}$ values increase for both charts but the Bayesian charts again have smaller $\text{SD}_{\text{CARL:in}}$ values. However, these values for the Bayesian t_r-chart become closer to each other for $m > 100$. This implies that, for $m > 100$, the Bayesian t_r-charts for each r provide similar IC performance.

An important issue related to the implementation of a control chart in case U is the size of the reference sample m. Clearly, large values of m are preferred (so, e.g.,, the $\text{SD}_{\text{CARL:in}}$ values would be small) but one must consider practical constraints. Zhang et al (2014) recommended that the $\text{SD}_{\text{CARL:in}}$ values be below 10% of the ARL_0 values in the known param-

TABLE 5. Performance Metrics for the Bayesian and Frequentist t_r-Charts ($r = 1, 2, 3$) for Different m and Nominal $ARL_0 = 370.4$

		Bayesian t_r-chart						Frequentist t_r-chart					
		$r=1$		$r=2$		$r=3$		$r=1$		$r=2$		$r=3$	
$a+m$	δ	AARL	SD_{CARL}	AARL	SD_{CARL}	AARL	SD_{CARL}	AARL	SD_{CARL}	AARL	SD_{CARL}	AARL	SD_{CARL}
20	5	124.4	29.2	31.3	14.4	11.2	6.9	175.6	41.3	48.3	22.6	17.7	11.6
	4	155.4	36.5	47.3	22.1	18.9	12.5	219.4	51.5	73.3	34.9	30.6	21.2
	3	207.0	48.4	81.1	38.6	38.7	27.2	292.1	67.8	126.6	60.6	64.3	46.1
	2	307.4	65.8	174.5	79.1	111.5	76.4	427.1	82.5	269.4	112.1	185.6	116.6
	1	**370.4**	**112.9**	**370.4**	**116.6**	**370.4**	**134.3**	**370.4**	**170.3**	**370.4**	**178.1**	**370.4**	**188.2**
	0.8	255.9	138.2	272.7	156.4	287.0	174.3	210.5	152.4	206.1	171.1	205.5	185.6
	0.6	107.5	90.1	104.0	107.0	103.1	121.0	74.1	70.5	59.8	73.7	52.3	76.6
	0.4	24.9	20.5	17.2	18.6	13.4	17.5	17.6	13.1	10.6	9.5	7.6	7.6
	0.2	4.8	1.8	2.8	1.0	2.0	0.7	4.0	1.3	2.3	0.7	1.7	0.4
100	5	140.4	14.1	32.9	6.1	10.9	2.5	154.4	15.6	37.1	7.0	12.3	2.9
	4	175.4	17.7	49.6	9.4	18.3	4.5	192.9	19.4	56.0	10.7	20.8	5.2
	3	233.7	23.6	85.1	16.5	37.2	9.8	257.0	25.9	96.4	18.7	42.8	11.4
	2	349.8	34.6	184.8	36.4	107.7	30.1	384.5	37.8	209.7	41.3	124.8	35.0
	1	**370.4**	**83.4**	**370.4**	**82.5**	**370.4**	**82.5**	**370.4**	**93.6**	**370.4**	**97.9**	**370.4**	**100.9**
	0.8	185.2	71.2	169.2	80.6	159.6	87.6	175.6	70.4	155.0	78.0	142.0	83.0
	0.6	58.8	23.4	40.9	20.1	31.6	17.6	55.0	21.8	37.1	17.9	27.9	15.2
	0.4	15.3	4.3	8.8	2.7	6.1	1.9	14.6	4.0	8.2	2.4	5.6	1.7
	0.2	3.9	0.5	2.2	0.3	1.7	0.2	3.8	0.5	2.2	0.3	1.6	0.2
500	5	146.6	6.5	33.7	2.8	10.9	1.1	149.8	6.7	34.7	2.9	11.2	1.1
	4	183.2	8.2	50.9	4.3	18.3	2.0	187.1	8.4	52.4	4.4	18.9	2.0
	3	244.0	10.9	87.4	7.4	37.3	4.3	249.3	11.2	90.0	7.7	38.5	4.4
	2	365.5	16.2	190.0	16.5	108.0	13.1	373.3	16.5	195.5	16.9	111.7	13.6
	1	**370.4**	**44.2**	**370.4**	**46.2**	**370.4**	**46.7**	**370.4**	**45.3**	**370.4**	**48.2**	**370.4**	**49.5**
	0.8	167.3	30.9	141.4	33.1	124.1	33.9	165.6	30.8	138.9	32.7	121.2	33.2
	0.6	52.0	8.9	33.8	6.8	24.8	5.5	51.4	8.7	33.3	6.7	24.3	5.3
	0.4	14.2	1.7	7.9	1.0	5.4	0.7	14.1	1.7	7.8	1.0	5.3	0.7
	0.2	3.8	0.2	2.2	0.1	1.6	0.1	3.8	0.2	2.1	0.1	1.6	0.1
∞	5	148.5	0.0	34.1	0.0	10.9	0.0	148.5	0.0	34.1	0.0	10.9	0.0
	4	185.6	0.0	51.4	0.0	18.4	0.0	185.6	0.0	51.4	0.0	18.4	0.0
	3	247.2	0.0	88.3	0.0	37.4	0.0	247.2	0.0	88.3	0.0	37.4	0.0
	2	370.4	0.0	191.8	0.0	108.2	0.0	370.4	0.0	191.8	0.0	108.2	0.0
	1	**370.4**	**0.0**	**370.4**	**0.0**	**370.4**	**0.0**	**370.4**	**0.0**	**370.4**	**0.0**	**370.4**	**0.0**
	0.8	162.8	0.0	134.5	0.0	115.5	0.0	162.8	0.0	134.5	0.0	115.5	0.0
	0.6	50.5	0.0	32.4	0.0	23.4	0.0	50.5	0.0	32.4	0.0	23.4	0.0
	0.4	14.0	0.0	7.7	0.0	5.2	0.0	14.0	0.0	7.7	0.0	5.2	0.0
	0.2	3.7	0.0	2.1	0.0	1.6	0.0	3.7	0.0	2.1	0.0	1.6	0.0

eter case (i.e., 370.4) in the classical setting. It is observed that the $SD_{CARL:in}$ values of the Bayesian t_r-chart fall below 10% of the ARL_0 values in the known parameter case when $m > 800$. This means that, in order to have a predictable IC performance of the Bayesian t_r-chart using, e.g., a noninformative prior, a large number of phase I observations (approximately 800) is required. This should not be considered as a disadvantage, however, because the same is true for the frequentist t_r-chart.

So far, we have examined the IC performance of the Bayesian t_r-chart for the noninformative prior. Of course, the intuitive advantage of the Bayesian

t_r-chart lies in incorporating any prior information from the past experience, along with the information from the available phase I sample, to improve process monitoring. We provide some observations to this end. Note that, as mentioned at the beginning of Section 6.1 and shown in the Appendix, the performance metrics of the proposed Bayesian t_r-chart depend on $(a+m)$ and thus the values of these metrics shown in Table 5 may be interpreted as the metrics corresponding to some informative priors. For example, the performance of the Bayesian t_r-chart for the informative $\Gamma(5, 95)$ prior, with $m = 95$, would be the same as that of the Bayesian t_r-chart for a $\Gamma(0, 0)$ prior (noninformative prior) with $m = 100$, because $(a + m)$ equals 100. In fact, each Bayesian t_r-chart having the same value of $(a + m)$ would have the same performance, regardless of the value of a.

One consequence of this equivalence is that, if a practitioner has some prior knowledge/information, the required number of phase I observations m may be reduced to get good chart performance. Intuitively, this means that the more information one has on the prior distribution, fewer phase I observations will be needed in order to get a similar chart performance compared with when there is no such information. For example, for the noninformative prior ($a = 0$, $b = 0$) and $m = 20$ (i.e., $a + m = 20$), the $\mathrm{SD}_{\mathrm{CARL:in}}$ for the t_3-chart is 134.4 whereas, for $a = 80$ and $m = 20$ ($a + m = 100$), the $\mathrm{SD}_{\mathrm{CARL:in}}$ value is 82.5.

It can also be observed from Table 5 that the performance of the Bayesian t_r-chart is sensitive to the shape parameter a of the prior distribution for a fixed phase I sample size. The stronger the belief of a practitioner about his prior, the larger is the value of a, implying better performance of the chart. It shows that incorporating more knowledge, the Bayesian t_r-chart gives more predictable $\mathrm{AARL}_{\mathrm{in}}$ values for a fixed number of phase I observations.

However, in practice, the practitioners might find themselves unable to specify the prior accurately and hence a weakly informative prior may be preferred where the parameters a and b are chosen such that the variance of the prior distribution is larger compared to the mean, in order to reflect the uncertainty around the prior belief about the mean a/b. Hence, in the case of a weakly informative prior, when the value of a is chosen to be too small, the performance of the chart is very close to the case of a noninformative prior.

6.2. Performance Comparison with the Frequentist t_r-Chart

It is of interest to examine the performance of the proposed Bayesian t_r-chart and we do that in this section. We first consider the case of the noninformative prior. Then we discuss the case when the practitioner has some prior information about the rate parameter so that a (different; informative) prior distribution can be used. Table 5 shows the results for both the $\mathrm{AARL}_{\mathrm{in}}$, $\mathrm{AARL}_{\mathrm{OOC}}$ (denoting the AARL value when the process is OOC), and the $\mathrm{SD}_{\mathrm{CARL:in}}$, $\mathrm{SD}_{\mathrm{CARL:ooc}}$ (denoting the $\mathrm{SD}_{\mathrm{CARL}}$ value when the process is OOC) values for the Bayesian t_r-chart ($r = 1, 2, 3$) using the noninformative prior and the frequentist t_r-chart, which are both designed so that each chart has the $\mathrm{AARL}_{\mathrm{in}}$ value equal to the nominal $\mathrm{ARL}_0 = 370.4$. We consider three different values of m (20, 100, 500) and assume that the rate parameter shifts, both high and low, according to δ ($\delta = 5$, 4, 3, 2, 1, 0.8, 0.6, 0.4, 0.2). As noted before, the values in the last block for $m = \infty$ for each chart are the corresponding values in case K. It should be noted that, for these cases, the $\mathrm{SD}_{\mathrm{CARL}}$ values are equal to zero because the CARL values all converge to the corresponding values in case K, which is a constant, and hence there is no variation in the CARL distribution.

According to the results shown in Table 5, the OOC performance of both the frequentist and the Bayesian charts are highly affected by the estimation error, which is introduced through the posterior distribution of λ in the case of the Bayesian t_r-chart and through the sampling distribution of λ in case of the frequentist t_r-chart. For example, for $m = 20$ and $\delta = 2$, the $\mathrm{AARL}_{\mathrm{OOC}}$ values of the Bayesian t_1-, t_2-, and t_3-charts are 307.4, 174.5, and 111.5, respectively, whereas for the frequentist t_1-, t_2-, and t_3-charts, the corresponding $\mathrm{AARL}_{\mathrm{OOC}}$ values are 427.1, 269.4, and 185.6, respectively. On the other hand, for case K, the OOC ARL values for these charts when $\delta = 2$ are 370.4, 191.8, and 108.2, respectively, so estimation does cause a delay in detection but the Bayesian charts have relatively better performance. For small values of m, the Bayesian t_r-chart (for $r = 1, 2, 3$) with a noninformative prior has much smaller $\mathrm{AARL}_{\mathrm{OOC}}$ and $\mathrm{SD}_{\mathrm{CARL:ooc}}$ values than the corresponding values of the frequentist t_r-chart for $\delta > 1$ (when the rate increases, so that the mean time between events decreases), i.e., the process deteriorates, which is the more serious and important case). For example, for $m = 20$, the

AARL_{OOC} is equal to 307.4 with $\text{SD}_{\text{CARL:ooc}}$ equal to 65.8 for the Bayesian t_1-chart using the noninformative prior when $\delta = 2$, whereas the corresponding values for the frequentist t_1-chart are 427.1 and 82.5, respectively. This implies that the Bayesian t_1-chart using a noninformative prior is more sensitive to the shift in the rate parameter when the process deteriorates than the corresponding frequentist t_r-chart. Even with the noninformative prior, the Bayesian t_r-chart has better performance (in terms of AARL_{ooc}) than the case K itself when the process deteriorates. For large $m \geq 500$, the AARL_{OOC} and $\text{SD}_{\text{CARL:ooc}}$ values for both Bayesian (with noninformative prior) and frequentist t_r-charts converge to the corresponding values in case K, still the Bayesian t_r-chart outperforms the frequentist t_r-chart when the process deteriorates. On the other hand, when the process improves, $\delta < 1$ (which is the less serious case), the Bayesian t_r-chart using a noninformative prior has higher AARL_{OOC} and $\text{SD}_{\text{CARL:ooc}}$ values than the frequentist t_r-chart for smaller values of $m \leq 500$. However, both charts have similar performance in terms of AARL_{OOC} and $\text{SD}_{\text{CARL:ooc}}$ values for $m > 500$ and $\delta < 1$.

In general, the AARL and the SD_{CARL} evaluations for the Bayesian chart using the noninformative prior and the frequentist t_r-charts reveal that the performances of both charts are seriously affected in case U, especially when the phase I sample size is small. However, the Bayesian t_r-chart using the noninformative prior is preferable for two reasons: first, when the process deteriorates, the Bayesian t_r-chart gives alarms more quickly (smaller AARL_{OOC} values) than the frequentist t_r-chart (even more quickly in case K) for all values of m; second, the Bayesian t_r-chart has more predictable (less variable; smaller $\text{SD}_{\text{CARL:in}}$ values) in-control performance than the frequentist t_r-chart. Furthermore, note that, for smaller values of m (< 100), the Bayesian t_r-chart using the noninformative prior has higher $\text{SD}_{\text{CARL:in}}$ values with higher values of r; however, when $m > 100$, the $\text{SD}_{\text{CARL:in}}$ values become close to each other for each Bayesian t_r-chart ($r = 1, 2, 3$). For example, when $m = 100$, the $\text{SD}_{\text{CARL:in}}$ values are 83.4, 82.5, 82.5 for the Bayesian t_1-, t_2-, and t_3-charts using noninformative priors, respectively. Hence, to improve the performance of the chart, the Bayesian t_r-chart using noninformative prior with higher values of r are recommended.

Note that we have compared the performance of the frequentist t_r-chart and the Bayesian t_r-chart using the noninformative prior in detail. Based on these findings, a few conclusions can be drawn in the informative prior case, which might require a more in-depth analysis to be taken up in a future work. As mentioned before, in Table 5, the values corresponding to $m = 20$, 100, 500 for the Bayesian t_r-chart are actually the values corresponding to $(a + m) = 20$, 100, and 500 when $a = 0$. For example, suppose one has $a = 80$ and $m = 20$, then the values for the Bayesian t_r-chart corresponding to $m = 100$ in Table 5 are comparable with the values of the frequentist t_r-chart corresponding to $m = 20$. Clearly, in case with available information about the parameter ($a > 0$), the Bayesian t_r-charts become better than the frequentist t_r-charts in terms of lower $\text{SD}_{\text{CARL:in}}$ values and even perform better with respect to AARL_{OOC} values. For example, when $a = 80$ and $m = 20$, the Bayesian t_1-chart has lower AARL_{OOC} and $\text{SD}_{\text{CARL:in}}$ values than the frequentist t_1-chart with $m = 20$ for all sizes of shift $\delta \neq 1$; also, the Bayesian t_1-chart has better predictable IC performance than the frequentist t_1-chart. It is also observed from Table 5 that, similar to IC chart performance, the OOC performance of the Bayesian t_r-chart is sensitive to the values of a and tends to the chart performance in case K. The AARL values become stabilized for $(a+m) > 500$, which shows that, for small phase I sample size, a large value of a (so that sum $(a + m)$ is approximately 500) is required to get a better performance close to the performance in Case K.

6.3. Performance Comparison with the Exponential CUSUM

So far, we have made comparisons between the Bayesian and the frequentist t_r-charts. There are other charts in the literature for monitoring the times between events with their pros and cons. Among them, the exponential CUSUM and the exponential EWMA charts are popular in practice for detecting smaller shifts. A separate and detailed study is necessary for a more complete comparison of the various TBE control charts in the unknown-parameter case. This is a topic for future research. Here, in order to provide some insight into the discussion and further highlight the effectiveness of the proposed Bayesian t_r-chart, we provide, in Table 6, a comparison between the Bayesian t_r-charts and the two-sided exponential CUSUM chart for monitoring times between events following the exponential distribution (Lucas (1985), Liu et al. (2006)). The exponential CUSUM chart is designed to be optimal for detecting

TABLE 6. Performance Metrics for the Bayesian and the Exponential CUSUM Chart for Different m and Nominal $ARL_0 = 370.4$

		Bayesian t_r-chart										
		$r=1$		$r=2$		$r=3$		$r=4$		Exponential CUSUM		
$a+m$	δ	AARL	SD_{CARL}	AARL	SD_{CARL}	AARL	SD_{CARL}	AARL	SD_{CARL}	AARL	SD_{CARL}	Design parameters
30	5	129.4	24.4	31.7	11.4	11.0	5.1	5.1	2.6	8.2	1.0	$H_L = 2.3876$,
	4	161.6	30.4	47.8	17.5	18.5	9.2	9.0	5.2	9.7	1.6	$H_U = 7.1350$
	3	215.3	40.5	82.0	30.6	37.8	20.1	20.5	13.5	13.7	4.3	
	2	321.0	56.9	177.4	65.4	109.6	59.9	74.0	52.9	39.7	32.1	
	1	**370.4**	**108.8**	**370.4**	**107.3**	**370.4**	**116.3**	**370.4**	**130.0**	**370.0**	**166.7**	
	0.8	230.4	122.4	237.0	139.8	244.5	154.8	250.9	168.6	229.8	179.4	
	0.6	84.7	62.8	72.8	69.2	66.3	74.4	61.7	78.6	60.1	81.5	
	0.4	20.0	12.0	12.6	9.2	9.2	7.5	7.2	6.4	11.6	7.5	
	0.2	4.3	1.2	2.5	0.7	1.9	0.4	1.5	0.3	3.7	0.8	
100	5	140.4	14.1	32.9	6.1	10.9	2.5	4.9	1.2	7.9	0.5	$H_L = 2.2792$,
	4	175.4	17.7	49.6	9.4	18.3	4.5	8.6	2.4	9.2	0.8	$H_U = 6.7573$
	3	233.7	23.6	85.1	16.5	37.2	9.8	19.2	6.0	12.8	2.0	
	2	349.8	34.6	184.8	36.3	107.7	30.1	68.5	23.8	32.2	11.9	
	1	**370.4**	**83.4**	**370.4**	**82.5**	**370.4**	**82.5**	**370.4**	**84.6**	**370.9**	**89.7**	
	0.8	185.2	71.2	169.2	80.6	159.6	87.6	152.5	93.2	156.7	94.2	
	0.6	58.8	23.4	40.9	20.1	31.6	17.6	25.7	15.7	32.4	15.4	
	0.4	15.3	4.3	8.8	2.7	6.1	1.9	4.6	1.4	9.3	2.0	
	0.2	3.9	0.5	2.2	0.3	1.7	0.2	1.4	0.1	3.4	0.3	
500	5	146.6	6.5	33.7	2.8	10.9	1.1	4.9	0.5	7.6	0.2	$H_L = 2.2211$,
	4	183.2	8.2	50.9	4.3	18.3	2.0	8.5	1.0	8.9	0.3	$H_U = 6.5544$
	3	244.0	10.9	87.4	7.4	37.3	4.3	18.9	2.5	12.1	0.8	
	2	365.5	16.2	190.0	16.5	108.0	13.1	66.9	9.9	28.5	3.9	
	1	**370.4**	**44.2**	**370.4**	**46.2**	**370.4**	**46.7**	**370.4**	**47.0**	**369.4**	**32.0**	
	0.8	167.3	30.9	141.4	33.1	124.1	33.9	111.0	33.9	126.9	36.6	
	0.6	52.0	8.9	33.8	6.8	24.8	5.5	19.3	4.5	28.6	5.3	
	0.4	14.2	1.7	7.9	1.0	5.4	0.7	4.0	0.5	8.9	0.8	
	0.2	3.8	0.2	2.2	0.1	1.6	0.1	1.3	0.0	3.3	0.2	

the shifts 10/3 and 1/3 times the IC parameter value respectively. These shifts for optimal design are also used by Liu et al (2006). The lower control limit H_L and upper control limits H_U are determined so that the exponential CUSUM chart attains the $AARL_{in}$ equal to the nominal ARL_0 (370.4). The values of H_L and H_U for $m = 30$, 100, and 500 are provided in Table 6. To compute the AARL and SD_{CARL} values for the two-sided exponential CUSUM chart, we followed Ozsan et al. (2010), by using Simpson's quadrature in MATLAB R2014a. Note that Zhang et al. (2014) also considered the exponential CUSUM chart but in the one-sided case.

We also calculated the AARL and SD_{CARL} values for the t_4-chart. Table 6 reveals that, for the noninformative prior (when $a = 0$), the Bayesian t_r-chart may be more attractive to the practitioner because lower $SD_{CARL:in}$ values are found for smaller values of $m \leq 100$. For example, when the phase I sample size is 30, the $SD_{CARL:in}$ value for exponential CUSUM chart is 166.7, whereas these are 108.8, 107.3, 116.3, and 130.0, respectively, for the t_1, t_2, t_3, and t_4 Bayesian charts, respectively. For the smaller values of $m \leq 30$, the exponential CUSUM chart outperforms only for smaller shift sizes ($0.8 < \delta < 3$) but, of course, the exponential CUSUM charts are designed to be more sensitive to the smaller shifts. However, interestingly, for larger values of $m \geq 100$, the t_4-chart outperforms the exponential CUSUM chart for almost all values of δ, except for smaller shifts $1 < \delta \leq 3$. On the other hand, when the prior in-

formation about λ is available, the Bayesian t_r-chart performs better than the exponential CUSUM chart as a increases. For large values of a, the Bayesian t_3- and t_4-charts become comparable with the exponential CUSUM chart except for $1 < \delta \leq 2$. However, note that, even though the exponential CUSUM charts are appealing in some cases, it can be quite complicated to implement in practice in terms of design (Liu et al. (2006)) relative to a Shewhart chart.

7. Summary and Conclusions

In this paper, we consider a Bayesian approach to construct the control limits of a Shewhart-type phase II t_r-chart for monitoring the times between events following an exponential distribution with an unknown rate parameter. The uncertainty in the unknown parameter is incorporated in the construction of the control limits by using a gamma prior distribution and utilizing the data from a fixed reference sample. The proposed control limits are probability limits based on the predictive distribution of a plotting statistic calculated from the phase II (test) sample of observations that is being monitored. The plotting statistic is taken to be the same as the one used in the frequentist case.

For the designed Bayesian t_r-chart to have the AARL_{in} value equal to the nominal ARL_0, it was observed that, in the case of the noninformative prior, the number of phase I observations required to have a reliable in-control chart performance was about 800. On the other hand, if one has prior information about the unknown rate parameter, this can be incorporated along with the information available from phase I observations in the Bayesian paradigm. In this case, it has been shown that the performance of the proposed Bayesian t_r-chart improves if a more informative (less variable) prior is used. When more prior information is available, which corresponds to taking a larger value of the shape parameter in the prior distribution, the $\text{SD}_{\text{CARL:in}}$ values decrease so that the practitioners have more confidence in the AARL_{in} values. In this case, one also requires a smaller number of phase I observations (compared with the case of a noninformative prior) to get the same level of desired IC performance.

It was also observed that, for larger amounts of phase I data (sample size), the Bayesian control limits converge to the control limits in the known-parameter case irrespective of the type of the gamma prior distribution used and the difference between the performances of the Bayesian and the frequentist t_r-charts becomes insignificant. This is reassuring for the practitioner. Furthermore, based on the performance comparison study between the Bayesian and frequentist t_r-chart, it was found that the Bayesian t_r-chart provides much better performance than the frequentist t_r-chart in the more serious case of a process deterioration, especially for a smaller phase I sample size, even though it has slightly higher AARL_{OOC} values in the less serious case when the process improves. The Bayesian t_r-chart is recommended, even when one has no prior information about the rate parameter, over the frequentist t_r-chart when the rate parameter is unknown, especially when a relatively smaller number of phase I observations is available. Our study also reveals that, for smaller phase I sample sizes (less than 100), the Bayesian t_r-charts have lower $\text{SD}_{\text{CARL:in}}$ values than the exponential CUSUM chart available in the literature and, hence, gives the users more confidence in their AARL_{in} values. Thus, the Bayesian t_r-charts may be preferred as they are easy to design and implement. On the other hand, the exponential CUSUM chart is more efficient especially for detecting smaller shifts; however, the performance of the Bayesian t_4-chart is comparable.

Finally, several problem areas can be explored in the future as follow-ups to this work. For example, in this paper, we considered the conjugate prior due to the ease in computations; however, other nonconjugate priors can be examined and studied. Also, the Shewhart chart is used for simplicity and overall performance, but consideration of other types of time-based charts for monitoring of interarrival times, such as the CUSUM and the EWMA, in the Bayesian framework, will be interesting and worth pursuing. A more comprehensive performance comparison of TBE charts, including self-starting charts, such as the Q charts (Quesenberry (1997)), will also be worthwhile.

Appendix A

Using Equation (5), the conditional probability of a signal for the frequentist t_r-chart in phase II (Kumar and Chakraborti (2016)) is given by

$$\begin{aligned}\beta_F(\hat{\lambda}) &= P[T_r < \hat{L}_r^M \text{ or } T_r > \hat{U}_r^M \mid \lambda_1] \\ &= 1 + G_{\chi^2_{2r}}(2\delta\lambda A_1^*/\hat{\lambda}) - G_{\chi^2_{2r}}(2\delta\lambda A_1^*/\hat{\lambda}),\end{aligned} \tag{A.1}$$

where $\lambda_1 = \delta\lambda$, δ being the size of the shift in the rate parameter λ, and the constants A_1^* and A_2^* are given in Equation (3).

Letting $W = 2m\lambda/\hat{\lambda}$, Equation (A.1) can be further written as

$$\beta_F(W) = 1 + G_{\chi^2_{2r}}(\delta A_1^* W/m) - G_{\chi^2_{2r}}(\delta A_2^* W/m).$$

Because $y = \sum_{i=1}^{m} x_i$ is the sum of the m phase I observations, it follows the $\Gamma(m, \lambda)$ distribution, which implies that $W = 2m\lambda/\hat{\lambda} = 2\lambda y$ follows a chi-square distribution with $2m$ degrees of freedom. Thus, the conditional probability of a signal is a function of a chi-square random variable and hence itself is a random variable. Further, when $\delta = 1$, the process is IC and the conditional probability of a signal is the conditional false alarm rate, CFAR. Thus,

$$\text{CFAR} = 1 + G_{\chi^2_{2r}}(A_1^* W/m) - G_{\chi^2_{2r}}(A_2^* W/m).$$

Following the line of arguments in Section 5, we can define the metrics AARL and SD_{CARL} for the frequentist t_r-chart as follows:

$$\text{AARL} = \int_0^\infty \frac{1}{\beta_F(w)} h(w)dw$$

$$\text{SD}_{\text{CARL}} = \sqrt{\int_0^\infty \frac{1}{\beta_F^2(w)} h(w)dw - \left(\int_0^\infty \frac{1}{\beta_F(w)} h(w)dw\right)^2},$$

where $h(w)$ is the density function of a chi-square distribution with $2m$ degrees of freedom. It can be easily shown that these metrics do not depend on λ but depend only on m, δ, and nominal ARL_0.

Appendix B

Theorem 1

When $a \to \infty$ such that the mean of the prior distribution of λ, i.e., $a/b \to \lambda_0$, the predictive density of T_r in Equation (6) converges to a gamma distribution with parameters r and λ_0. Hence, under these conditions, the distribution of $2\lambda_0 T_r$ converges to a chi-square distribution with $2r$ degrees of freedom.

Proof

The predictive density in Equation (6) can be rewritten as

$$f_{T_r|y}(t) = \frac{t^{r-1}}{\Gamma(r)} \cdot \frac{\Gamma(a+m+r)}{\Gamma(a+m)(b+y)^r} \cdot \frac{1}{\left[1+\frac{t}{b+y}\right]^{a+m+r}}; \quad t > 0$$

$$= \frac{t^{r-1}}{\Gamma(r)} \cdot \frac{\Gamma(a+m+r)}{\Gamma a a^{m+r}} \cdot \frac{\Gamma a a^m}{\Gamma(a+m)} \cdot \left(\frac{a}{b+y}\right)^r \cdot \frac{1}{\left[1+\frac{a}{b+y}\frac{t}{a}\right]^{a+m+r}}.$$

Because $a \to \infty$ and $a/b \to \lambda_0$, we have $a/(b+y) \to \lambda_0$. Also, using the results

$$\lim_{x\to\infty} \frac{\Gamma(x+r)}{\Gamma(x)x^r} = 1 \text{ and } \lim_{n\to\infty} \left(1+\frac{x}{n}\right)^n = e^x,$$

we get

$$\lim_{a\to\infty} f_{T_r|y}(t) = \frac{\lambda_0^r}{\Gamma(r)} t^{r-1} e^{-\lambda_0 t}; \quad t > 0$$

Hence, as $a \to \infty$ and $a/b \to \lambda_0$, the distribution of $2\lambda_0 T_r$ converges to a chi-square distribution with $2r$ degrees of freedom.

Theorem 2

When $m \to \infty$, the predictive density in Equation (6) converges to a gamma distribution with parameters r and λ, for all gamma priors (i.e., for all a and b). Hence, when $m \to \infty$, the distribution of $2\lambda T_r$ converges to a chi-square distribution with $2r$ degrees of freedom.

Proof

It is well known that, when the sample size $m \to \infty$, the ML estimator converges to the parameter. Thus $m/y \to \lambda$ as $m \to \infty$. Now, the predictive density in Equation (6) can be re-expressed as

$$f_{T_r|y}(t) = \frac{t^{r-1}}{\Gamma(r)} \cdot \frac{\Gamma(a+m+r)}{\Gamma(a+m)(b+y)^r} \cdot \frac{1}{\left[1+\frac{t}{b+y}\right]^{a+m+r}}; \quad t > 0$$

$$= \frac{t^{r-1}}{\Gamma(r)} \cdot \frac{\Gamma(a+m+r)}{\Gamma(m)m^{a+r}} \cdot \frac{\Gamma m m^a}{\Gamma(m+a)} \cdot \left(\frac{m}{b+y}\right)^r \cdot \frac{1}{\left[1+\frac{m}{b+y}\frac{t}{m}\right]^{a+m+r}}.$$

Now, when $m \to \infty$, $m/(b+y) \to \lambda$. Hence, following the line of arguments in the previous theorem, we have

$$\lim_{a\to\infty} f_{T_r|y}(t) = \frac{\lambda^r}{\Gamma(r)} t^{r-1} e^{-\lambda t}. \quad t > 0$$

Hence, as $m \to \infty$, $2\lambda T_r$ follows a chi-square with $2r$ degrees of freedom.

Appendix C

The metric AARL can be written using Equations (8) and (9) as

$$\text{AARL} = \int_0^\infty \frac{1}{1 + G_{\chi^2_{2r}}(2\delta\lambda(b+y)B_1) - G_{\chi^2_{2r}}(2\delta\lambda(b+y)B_2)} \cdot \frac{(b+y)^{a+m}}{\Gamma(a+m)}\lambda^{a+m-1}e^{-(b+y)\lambda}d\lambda,$$

where

$$B_1 = \left(\frac{1}{B_{1-\alpha_B/2}(a+m,r)} - 1\right)$$

and

$$B_2 = \left(\frac{1}{B_{\alpha_B/2}(a+m,r)} - 1\right).$$

Making a transformation $z = (b+y)\lambda$ with jacobian $= 1/(b+y)$, the expression for AARL reduces to

$$\text{AARL} = \int_0^\infty \frac{1}{[1 + G_{\chi^2_{2r}}(2\delta z B_1) - G_{\chi^2_{2r}}(2\delta z B_2)]} \cdot \frac{1}{\Gamma(a+m)}z^{a+m-1}e^{-z}dz.$$

It follows that the metric AARL and likewise the other metrics in Equations (12) and (13) do not depend on λ, y, and b and they are the functions of a, m, δ, and ARL_0 only.

Acknowledgments

The authors would like to thank two anonymous reviewers and the Editor for their helpful and constructive comments that have improved the paper. The first author's work was supported by a postdoctoral fellowship from the South African Research Chairs Initiative (SARChI) award. Partial support was also provided by the Department of Statistics, University of Pretoria.

References

Arnold, B. F. (1990). "An Economic $\overline{X}$-Chart to the Joint Control for the Means of Independent Quality Characteristics". *Zeitschrift für Operations Research* 34, pp. 59–74.

Bayarri, M. J.; Berger, J. O.; Forte, A.; and García-Donato, G. (2012). "Criteria for Bayesian Model Choice with Application to Variable Selection". *Annals of Statistics* 40, pp. 1550–1577.

Berger, J. O. (1985). *Statistical Decision Theory and Bayesian Analysis*, 2nd ed. New York, NY: Springer-Verlag.

Borror, C. M.; Kates, J. B.; and Montgomery, D. C. (2003). "Robustness of the Time Between Events CUSUM". *International Journal of Production Research* 41, pp. 3435–3444.

Chan, L. Y.; Lin, D. K. J.; Xie, M.; and Goh, T. N. (2002). "Cumulative Probability Control Charts for Geometric and Exponential Process Characteristics". *International Journal of Production Research* 40, pp. 133–150.

Chen, G. (1997). "The Mean and Standard Deviation of the Run Length Distribution of $\overline{X}$ Charts when Control Limits Are Estimated". *Statistica Sinica* 7, pp. 789–798.

Cheng, C. S. and Chen, P. W. (2011). "An ARL-Unbiased Design of Time-Between-Events Control Charts with Runs Rules". *Journal of Statistical Computation and Simulation* 81, pp. 857–871.

Colosimo, B. M. and del Castillo, E. (2007). *Bayesian Process Monitoring, Control and Optimization*. Boca Raton, FL: Chapman and Hall/CRC.

Cowles, M. K. (2013). *Applied Bayesian Statistics with R and OpenBUGS Examples*. New York, NY: Springer.

Gan, F. F. (1994). "Design of Optimal CUSUM Control Charts". *Journal of Quality Technology* 26, pp. 109–124.

Gan, F. F. (1998). "Designs of One and Two-Sided Exponential EWMA Charts". *Journal of Quality Technology* 30, pp. 55–69.

Gelman, A. (2002). *Prior Distribution in Encyclopedia of Environmetrics*, vol. 3, El-Shaarawim, A. H. and Piegorsch, W. W., eds. Chichester, UK: John Wiley & Sons.

Ghosh, B. K.; Reynolds, M. R., Jr.; and Hui, Y. V. (1981). "Shewhart $\overline{X}$-Charts with Estimated Process Variance". *Communications in Statistics—Theory and Methods* 10, pp. 1797–1822.

Jarrett, R. G. (1979). "A Note on the Intervals Between Coal-Mining Disasters". *Biometrika* 66, pp. 191–193.

Jones, L. A. and Champ, C. W. (2002). "Phase I Control Charts for Times Between Events". *Quality and Reliability Engineering International* 18, pp. 479–488.

Jones, M. A. and Steiner, S. H. (2012). "Assessing the Effect of Estimation Error on the Risk-Adjusted CUSUM Chart Performance". *International Journal for Quality in Health Care* 24, pp. 176–181.

Kass, R. E. and Wasserman, L. (1996). "The Selection of Prior Distributions by Formal Rules". *Journal of American Statistical Association* 91, pp. 1343–1370.

Kumar, N. and Chakraborti, S. (2015). "Improved Phase I Control Charts for Monitoring Times Between Events". *Quality and Reliability Engineering International* 31, pp. 659–668.

Kumar, N. and Chakraborti, S. (2016). "Phase II Shewhart-Type Control Charts for Monitoring Times Between Events and Effects of Parameter Estimation". *Quality and Reliability Engineering International* 32, pp. 315–328.

Liu, J. Y.; Xie, M.; Goh, T. N.; and Ranjan, P. (2004). "Time-Between-Events Charts for On-line Process Monitoring". In *Proceedings of the IEEE International Engineering Management Conference (IEMC '04)*, pp. 1061–1065.

Liu, J. Y.; Xie, M.; Goh, T. N.; and Sharma, P. R. (2006). "A Comparative Study of Exponential Time Between Events Charts". *Quality Technology and Quantitative Management* 3, pp. 347–359.

Lucas, J. M. (1985). "Counted Data CUSUMs". *Technometrics* 27, pp. 129–144.

Menzefricke, U. (2002). "On the Evaluation of Control Chart Limits Based on Predictive Distributions". *Communication in Statistics—Theory and Methods* 31, pp. 1423–1440.

Montgomery, D. C. (2012). *Introduction to Statistical Quality Control*, 7th ed. Hoboken, NJ: John Wiley.

Nenes, G. and Tagaras, G. (2007). "The Economically Designed Two-sided Bayesian $\overline{X}$ Control Chart". *European Journal of Operational Research* 183, pp. 263–277.

Ozsan, G.; Testik, M. C.; and Weiss, C. H. (2010). "Properties of the Exponential EWMA Chart with Parameter Estimation". *Quality and Reliability Engineering International* 26, pp. 555–569.

Qu, L.; Wu, Z.; Rahim, A.; and Khoo, M. B. C. (2015). "A Balanced Two-sided CUSUM Chart for Monitoring Time Between Events". *European Journal of Industrial Engineering* 9, pp. 1–26.

Quesenberry, C. P. (1993). "The Effect of Sample Size on Estimated Limits for $\overline{X}$ and X Control Charts". *Journal of Quality Technology* 25, pp. 237–247.

Quesenberry, C. P. (1997). *SPC Methods for Quality Improvement*. New York, NY: John Wiley & Sons.

Raubenheimer, L. and Van der Merwe, A. J. (2015). "Bayesian Control Chart for Nonconformities". *Quality and Reliability Engineering International* 31, pp. 1359–1366.

Saleh, N. A.; Mahmoud, M. A.; and Abdel-Salam, A. S. G. (2013). "The Performance of the Adaptive Exponentially Weighted Moving Average Control Chart with Estimated Parameters". *Quality and Reliability Engineering International* 29, pp. 595–606.

Saleh, N. A.; Mahmoud, M. A.; Keefe, M. J.; and Woodall, W. H. (2015). "The Difficulty in Designing Shewhart $\overline{X}$ and X Control Charts with Estimated Parameters". *Journal of Quality Technology*, 47 pp. 127–138.

Tsiamyrtzis, P. and Hawkins, D. M. (2007). "Statistical Process Control, Bayesian". In *Encyclopedia of Statistics in Quality and Reliability*. New York, NY: John Wiley & Sons.

Vardeman, S. and Ray, D. (1985). "Average Run Lengths for CUSUM Schemes when Observations Are Exponentially Distributed". *Technometrics*, 27 pp. 145–150.

Woodward, P. W. and Naylor, J. C. (1993). "An Application of Bayesian Methods in SPC". *The Statistician* 42, pp. 461–469.

Xie, M.; Goh, T. N.; and Ranjan, P. (2002). "Some Effective Control Chart Procedures for Reliability Monitoring". *Reliability Engineering and System Safety* 77, pp. 143–150.

Zhang, C. W.; Xie, M.; Liu, J. Y.; and Goh, T. N. (2007). "A Control Chart for the Gamma Distribution as a Model of Time Between Events". *International Journal of Production Research* 45, pp. 5649–5666.

Zhang, C. W.; Xie, M.; and Goh, T. N. (2006). "Design of Exponential Control Charts Using a Sequential Sampling Scheme". *IIE Transactions* 38, pp. 1105–1116.

Zhang, H. Y.; Shamsuzzaman, M.; Xie, M.; and Goh, T. N. (2011). "Design and Application of Exponential Chart for Monitoring Time-Between-Events Data Under Random Process Shift". *The International Journal of Advanced Manufacturing Technology* 57, pp. 849–857.

Zhang, M.; Megahed, F. M.; and Woodall, W. H. (2014). "Exponential CUSUM Charts with Estimated Control Limits". *Quality and Reliability Engineering International* 30, pp. 275–286.